HHS Public Access

Author manuscript

Biomaterials. Author manuscript; available in PMC 2018 September 01.

Published in final edited form as:

Biomaterials. 2017 September ; 140: 79–87. doi:10.1016/j.biomaterials.2017.06.017.

Macrophages with cellular backpacks for targeted drug delivery to the brain

Natalia L. Klyachko[a,b,c,1], **Roberta Polak**[d,e,1], **Matthew J. Haney**[a,b], **Yuling Zhao**[a,b], **Reginaldo J. Gomes Neto**[d,e], **Michael C. Hill**[d,e], **Alexander V. Kabanov**[a,b,c], **Robert E. Cohen**[d], **Michael F. Rubner**[d], and **Elena V. Batrakova**[a,b,*]

[a]Center for Nanotechnology in Drug Delivery, University of North Carolina at Chapel Hill, Chapel Hill, NC, USA

[b]Eshelman School of Pharmacy, University of North Carolina at Chapel Hill, Chapel Hill, NC, USA

[c]Department of Chemical Enzymology, Faculty of Chemistry, M.V. Lomonosov Moscow State University, Moscow, Russia

[d]Department of Chemical Engineering, Massachusetts Institute of Technology, Cambridge, MA, USA

[e]Department of Materials Science and Engineering, Massachusetts Institute of Technology, Cambridge, MA, USA

Abstract

Most potent therapeutics are unable to cross the blood-brain barrier following systemic administration, which necessitates the development of unconventional, clinically applicable drug delivery systems. With the given challenges, biologically active vehicles are crucial to accomplishing this task. We now report a new method for drug delivery that utilizes living cells as vehicles for drug carriage across the blood brain barrier. Cellular backpacks, 7–10 μm diameter polymer patches of a few hundred nanometers in thickness, are a potentially interesting approach, because they can act as drug depots that travel with the cell-carrier, without being phagocytized. Backpacks loaded with a potent antioxidant, catalase, were attached to autologous macrophages and systemically administered into mice with brain inflammation. Using inflammatory response cells enabled targeted drug transport to the inflamed brain. Furthermore, catalase-loaded backpacks demonstrated potent therapeutic effects deactivating free radicals released by activated microglia *in vitro*. This approach for drug carriage and release can accelerate the development of new drug formulations for all the neurodegenerative disorders.

*Corresponding author. UNC Eshelman School of Pharmacy, University of North Carolina at Chapel Hill, Chapel Hill, NC, 27599-7362, USA. batrakov@email.unc.edu (E.V. Batrakova).

[1]Authors equally contributed.

Author contributions

All authors contributed to writing and discussion.

Competing financial interests

The authors declare no competing financial interests.

Appendix A. Supplementary data

Supplementary data related to this article can be found at http://dx.doi.org/10.1016/j.biomaterials.2017.06.017.

Keywords

Catalase; Macrophages; Inflammation; Cell-mediated drug delivery; Layer-by-layer patches

1. Introduction

The delivery of therapeutics across the blood brain barrier (BBB) has been extremely challenging and is currently a major impediment for the treatment of diseases in the brain. Recently, living cells have been investigated as carriers for actively targeted drug delivery, which has opened new therapeutic avenues within the central nervous system (CNS) [1]. For this strategy to be successful, the efficient penetration across the BBB by cell-carriers is crucial for the success of these cell-based formulations. Some cell types are naturally capable of crossing the BBB, such as leukocytes (neutrophils and monocytes), which can traverse the endothelial wall due to increased margination and extravasation [2] when the BBB breaks down during inflammation [3–6]. These cells appear to traffic primarily between adjacent endothelial cells through the transient opening of tight junctions [7,8], and utilizing diapedesis and chemotaxis [9]. Because of their natural recruitment across the BBB during inflammation, immune cells are an ideal candidate as cellular vehicles for drug delivery.

For maximal efficacy, immune cells should carry therapeutically significant quantities of drug. Traditional strategies often result in poor drug loadings because they are sequestered within the phagosome of macrophages, which potentially degrades the drug and reduces the release rates. Furthermore, accumulated drugs, especially antineoplastic agents, may degrade the survival or migration of the cell-carrier [10], which has created a bottleneck for cell-based therapy. In addition, the small size of payload materials traversing the BBB with cell carriers can limit the amount delivered, with 100–200 nm particles currently being the largest [11]. To circumvent these limitations, cellular backpacks, micron-scale patches of a few hundred nanometers in thickness, were fabricated by layer-by-layer (LbL) assembly to be attached to the surface of cell-carriers [12–14]. Due to their shape, size and composition, cellular backpacks are not engulfed by macrophages, making them an attractive strategy that sequesters the cargo outside the cells to protect both the cell and the drug from degradation. Recent work has demonstrated that backpack-monocyte conjugates migrate and accumulate in inflamed tissue sites (e.g. lungs and skin) [15]. These cellular backpacks can be designed to carry toxic loads of a potent anticancer drug without affecting cell's natural functions [16]. Furthermore, cell backpacks loaded with catalase have shown antioxidant properties *in vitro* [17].

In this work, we introduce a new method that allows for noninvasive, safe and efficient access to most secluded sites in the brain. This strategy can be used for treatment of various neurodegenerative disorders, infectious diseases, and other types of brain and cellular injuries. We demonstrate that backpacks loaded with catalase can be attached to macrophages and transported across the BBB in a mouse model of lipopolysaccharide (LPS)-induced encephalitis. This indicates that engaging natural immune cells such as

monocyte-macrophages as drug carriers is a potentially new strategy for treating a range of neuroinflammatory and neurodegenerative diseases.

2. Results

2.1. Cell backpacks

Backpacks were constructed by a combination of photolithography and layer-by-layer (LbL) assembly [14], which resulted in disc-shaped polymer patches 7 μm in diameter. As shown in Fig. 1, the cell backpacks were initially fabricated by deposition of various material regions, serially, onto a glass microscope slide. At the interface between the glass slide and the assembled multilayer construct is a “release region” which can dissolve upon incubation with the sugar, melibiose. We had previously developed this as a simple and benign means to releasing backpacks from their substrates [18]. Atop this sacrificial film, we deposited a “magnetic region” to aid in purification of cell backpacks, confer film rigidity and potentially serve as an imaging agent [19–22]. Then we deposited a “payload region” that, in this case, contains catalase, a potent anti-oxidant (More details about catalase payload region can be found in Supplemental Fig. 1). Finally, the top layer is composed of a “cell attachment region”, which contains antibodies that enable the backpacks to specifically attach to desired cell-types. In this instance, we attached macrophage-targeting polyclonal antibodies through avidin-biotin links. Catalase-loaded backpacks could withstand the fabrication processing (See more details on Supplemental Fig. 2).

2.2. Ability for backpacks to cross the BBB in vitro

Cell backpacks were attached to macrophages as follows. Fluorescently-labeled DiO-macrophages (green, 2×10^6 cells/ml) were pipetted onto the surfaces of glass slides with fabricated cell backpacks, which were functionalized with NeutrAvidin Dylight 550 (red). After a brief incubation, macrophages adhered to the backpacks via CD11b antibody attachment, and the glass slides were thrice washed with media to remove non-adhered cells. (See online methods for more details; Supplemental Fig. 3). To detach the macrophage-backpack conjugates, the glass slides were incubated with 1 mL of 100 mM melibiose in PBS for 1 h at 37 °C[18]. The remaining weakly adhered macrophage-backpack conjugates were removed with a cell scraper and re-suspended into saline-buffered solution.

Fig. 2 shows microscope images of macrophages with attached backpacks. For this purpose, macrophages were labeled with a fluorescent dye DiO (green) and pipetted onto the surface of the glass slide with backpacks stained with Neutravidin Dylight 550 (red). Non-adhered cells were removed by rinsing with PBS, and backpack attached macrophages were detached from the glass slide using melibiose. The released cells with backpacks were seeded onto a slide and examined by confocal microscopy. The functionalization protocol yielded 80% conjugation. Noteworthy, backpacks did not affect macrophage viability (Supplemental Fig. 4).

A preliminary *in vitro* test was carried out to show whether cell backpacks were able to cross a cell monolayer. Backpacks alone and those attached to macrophages were incubated in a transwell plate containing a cell monolayer of mouse brain endothelial cells (bEnd.3), and

chemoattractant, macrophage chemotactic factor-1 (MCP-1) (150 ng/ml, R&D Systems) that was placed into the lower chamber [19]. Following incubation at 37 °C in a shaker, the bEnd.3 inserts were removed, placed in 24-well plates with fresh media, and centrifuged to pellet the migrating cells to the plate's bottom chamber (See online methods for details). As shown in Fig. 3, some backpacks were able to cross the cell monolayer *in vitro*, but significantly more could do so when attached to macrophages (Fig. 3A), meaning that the macrophages can work by facilitating the passage of backpacks through the BBB. The macrophages themselves are able to cross the cell monolayer *in vitro* and the added bulk from the cell backpacks slightly slows their transfer (Fig. 3B).

2.3. Recruitment of macrophages with the attached backpacks to the brain in LPS-intoxicated mice

To determine whether the macrophages were capable of carrying the cell backpacks across the blood-brain barrier *in vivo*, we used C57/BL mice with LPS-induced brain inflammation as described earlier [23]. Twenty-four hours later, freshly prepared macrophage-backpack conjugates were administered intravenously (5×10^6 cells/mouse in 100 μl). Fourteen hours later, mice were sacrificed, perfused, brains were sectioned, and examined by confocal microscopy. LPS-intoxicated mice injected with backpacks alone (no macrophages) were used as a control group. As shown in Fig. 4A, many macrophage aggregates (green) can be seen all over the brain. Noteworthy, only macrophage aggregates can be observed in that image (single macrophages or single backpacks cannot be observed). To better visualize whether backpacks were present in the brain, zoomed in images (40×) were acquired. Fig. 4C–**E** shows co-localization of fluorescently-labeled macrophages (green) and backpacks (red) manifested in white staining (shown by arrows). These images confirmed that macrophages delivered considerable amounts of backpacks to the inflamed brain. Noteworthy, loading macrophages with backpacks slightly slow down their transport to the brain (Supplemental Fig. 5) that was consistent with the results of *in vitro* transport experiment (Fig. 3B). No fluorescence was found in the inflamed brain when backpacks were injected alone (without cells) indicating that systemically administered macrophages accomplished transport of backpacks cross the BBB in the presence of brain inflammation (Fig. 4B).

2.4. Use of cell backpacks for drug delivery across the BBB

The ability of the macrophages to facilitate delivery of the cell backpacks across the BBB, suggests a new versatile platform for drug delivery. As described in Fig. 1, the backpacks were assembled to contain the enzyme catalase because of its antioxidant properties and potential for treating brain inflammation [24–27]. Although the payload region in this case was customized for catalase assembly, the versatility of LbL assembly enables the loading of a variety of therapeutics ranging from small molecules, to peptides and proteins [16,28–33]. With our catalase-loaded cell backpacks, we characterized their physical properties and biochemical activity. After film assembly, the total thickness (prior to release from the substrate) was ~600 nm. Separate measurements of the film growth of (CAT9.0/PAH9.0) films (Supplemental Fig. 1) reveal that this payload region is roughly 250 nm, indicating that a large fraction (~43%) of the backpack contains catalase. Furthermore, the maximal amount of catalase is loaded at 30 bilayers (Supplemental Fig. 1B). We quantified the activity of

catalase in the cell backpacks *via* decomposition of hydrogen peroxide and found 2.3 μU/cell backpack.

Fig. 5A shows that catalase freely dissolved in solution is readily deactivated when exposed to protease (~80% deactivation). Over 50% deactivation of catalase is also observed when (PAH9.0/CAT9.0) 30.5 films, representing the payload region, were incubated with protease. Interestingly, catalase contained in the backpacks is protected against protease degradation, exhibiting only ~40% deactivation. This fact can be explained by the presence of the cell-adhesive region placed on the top of the catalase containing payload region. Past works demonstrate that LbL films deposited onto catalase-contained nanoparticles are able to inhibit molecules larger than 5 nm from penetrating through the multilayer, thereby protecting the catalase against proteolysis [34,35]. In this case, the top of the payload is protected by the adhesive region, but the sides of the backpacks expose some of the catalase that are packed inside the backpacks, making them available to protease attack. To test this hypothesis we assembled the full backpack structure [(BSM/JAC)60 + (PAH/MNP)10.0 + (PAH/CAT)30 + (PAA/PAH-biotin)10] on a non-patterned slide. Non-patterned backpack films showed improved protection of the payload (catalase) (Supplemental Fig. 6).

The release of catalase from pre-loaded cell backpacks was evaluated by enzymatic activity using dialysis membranes with a cut off 2000 KDa (Fig. 5B–C). A prolonged and sustained release was recorded; less than 50% of catalase was released over 18 h (Fig. 5B). Furthermore, when incorporated into backpacks, catalase was stable over 42 days (Fig. 5C); about 60% and 75% of the catalase activity in backpacks was retained when stored at 4 °C and −20 °C, respectively.

Noteworthy, the attachment of the backpacks to the cell-carriers did not result in their activation and excessive production of Reactive Oxygen Species (ROS) into the media (Supplemental Fig. 7).

2.5. Modulation of ROS released by activated microglia

To assess the antioxidant capacity of the catalase-loaded cell backpacks on microglial ROS production, macrophages with attached empty or catalase-loaded backpacks were incubated for 2 h in Krebs-Ringer buffer, and the reluctant supernatant was then collected and added to tumor necrosis factor (TNF-α)-stimulated microglial cells (200 ng/ml). The catalase in the supernatants collected from the catalase-loaded macrophages decomposed hydrogen peroxide produced by activated microglia (Fig. 6). Furthermore, the supernatants collected from empty cell backpacks, or non-loaded macrophages (Supplemental Fig. 8) had little, if any effect on hydrogen peroxide levels. Altogether, this study suggests that cells with catalase-loaded patches can attenuate oxidative stress resulting from activation of microglia.

3. Discussion

We report here the use of a macrophage-based formulation that might serve as treatment of neurodegenerative disorders, that include Parkinson's and Alzheimer diseases (PD and AD), HIV-associated neurocognitive disorders [37,38], and stroke [39,40]. It was reported that

these disorders, are accompanied with brain inflammation [41] and excessive production of free radicals that are toxic to neurons [42–45].

The tendency of monocytes and macrophages to migrate to sites of inflammation makes them attractive candidates for use as vehicles to attenuate inflammation. We demonstrated earlier that systemically administered inflammatory cells home to regions of inflammation and neurodegeneration, accumulate at therapeutically relevant numbers, and deliver therapeutics to the inflamed mouse brain [26,27,46–49]. This property allow efficient disease treatment along with reductions in tissue toxicities and side effects.

Backpacks loaded with different types of cargo (e.g. enzymes, antibiotics, anti-inflammatories, anticancer drugs) can be conjugated to the surface of living cells (e.g. macrophages, lymphocytes, monocytes). The cell-backpack conjugate is then used as targeted drug-delivery system, since cell motility enables a targeted delivery that would not otherwise be achievable. Most importantly, attachment to macrophages enables the non-invasive delivery of drugs to sites of inflammation, especially across the BBB, a significant obstacle to drug treatment by traditional means such as systemic drugs. Furthermore, we demonstrated here that attachment of cell backpacks to macrophages did not alter their major functions, including adherence capability, or cell activation. However, it may affect trafficking backpack-laden macrophages to the brain. Indeed, micropatches conjugated to the cell-carriers may slow-down macrophage transport across the BBB due to the increased size. Nevertheless, the possibility of loading large amounts of therapeutics into the micropatches, along with sustained release and minimized drug exposure to the cell-carriers, provides a remarkable advantage over common strategies. Indeed, we confirmed that significant amount of backpack-laden macrophages were able to target and deliver cell backpacks to the inflamed brain tissues. We suggest that the large contact area between a backpack and cell-carrier, and strong antibody-mediated binding to macrophages result in extraordinary stability of the construct *in vivo* that allows macrophages efficiently penetrate across the cell monolayers without losing their cargo.

We utilize in this study one of the most potent antioxidants in nature, catalase. The means for successful therapy of such disorders by attenuating free radicals production has met with limited success based, in part, due to inefficient enzyme delivery to the affected brain regions and across the BBB [50]. As such, an efficient delivery of catalase to the brain may be instrumental for PD therapy. To accomplish macrophage-mediated delivery to the brain, we developed a method where catalase was incorporated into cell backpacks without losing its enzymatic activity, and then drug-loaded patches were attached to the cell-carriers. Catalase incorporated into backpacks reduced neuroinflammatory responses *in vitro* providing a translational link of these formulations to the clinic. Furthermore, we demonstrated that macrophages with attached backpacks facilitated their transport to the inflamed brain in a mouse model of LPS-induced encephalitis. We suggest that engaging natural immune cells such as monocyte/macrophages as drug carriers provides a new perspective for a range of different neuroinflammatory and neurodegenerative diseases.

Using the inflammation as a driving force for targeted cell-mediated drug delivery is a very attractive approach. Nevertheless, one should take into consideration that any other

inflammatory processes in addition to the CNS inflammation may divert cell-carriers from the brain and decrease the therapeutic efficacy of cell-incorporated drug formulations. In clinic, if this is the case, a short pre-treatment of a patient with antibiotics should be carried out before the cell-based therapy is initiated.

4. Online methods

4.1. Materials

CAT: Catalase from bovine liver was purchased from Calbiochem (San Diego, CA), or from Sigma-Aldrich; PAH: Poly(allylamine hydrochloride), MW 120–200 g/mol (for the magnetic region). PAA: Poly(acrylic acid) MW 200,000 g/mol 25% soln. In water (Polysciences). MNP: Magnetic nanoparticles, EMG 705 from FerroTec, 10 nm in diameter particles. BSM: bovine submaxillary mucin (Sigma). JAC: lectin jacalin (Vector Laboratories). TRIS: Tris(hydroxymethyl)aminomethane (Sigma-Aldrich). NHS-Biotin: (+)-Biotin N-hydroxysuccinimide ester (Sigma Aldrich). Positive photoresist S1813, MicroChem. Developer MF319. Micro BCA reagent (Thermo Fisher). 6-Hydroxydophamine (6-OHDA), lipopolysaccharides (LPS), and Triton X-100 were from Sigma-Aldrich (St. Louis, MO, USA). Interferon gamma (INF-γ) was purchased from Peprotech Inc. (RockyHill, NJ).

4.2. Cellular backpacks fabrication

Backpacks were fabricated according to previous works [12,14]. Briefly, a clean glass slide was spin-coated with a photoresist (S1813 positive photoresist, MicroChem) layer. Next, the photoresist is soft-baked to evaporate the solvent and then placed in a custom-made device that holds a photomask and a UV lamp. The parts exposed to the UV lamp are then removed by soaking the glass slide in a developer (MF319) solution, which will generate a photo-patterned slide. The patterned substrate contains circular areas of 7 μm diameter holes and 15 μm edge-to-edge spacing. The next step is to conformally coat the patterned slide with the desired multilayer films using LbL, and then dissolve the remaining parts of the photoresist to leave the backpacks attached to the glass slide.

4.3. Multilayer thin films

The backpacks are comprised of 4 different regions. The first region deposited is called the releasable region and is composed of $(BSM7.4/JAC7.4)_{60}$ [18]. Next, a magnetic region of $(PAH3/MNP4)_{10.5}$ is deposited on the top of the releasable region to add rigidity [51]. The payload region is assembled on the top of the magnetic region and is comprised of $(CAT9.0/PAH9.0)_{30}$. Both PAH (1 mg/mL) and CAT (0.5 mg/mL) were dissolved in TRIS buffer 20 mM pH 9.0. Deposition times for both CAT and PAH was of 10 min, followed by two rinse steps of 2 and 1 min each. Rinse steps were performed using TRIS buffer (20 mM, pH 9.0). Details on catalase multilayer film choice will be published in a separate manuscript. Lastly, the samples were topped with the adhesive region, composed of $(PAA4.0/PAH\text{-}biotin4.0)_{10}$ [52]. Note that all the solutions were freshly prepared and used on the same day.

4.4. Antibody attachment

Samples 50 μg/mL NeutrAvidin Dylight 633 in pH 7.4 PBS buffer for 1 h at 4 °C. Glass slides are rinsed three times in PBS. Backpacks are then incubated with biotinylated antibody (50 μg/mL) diluted with PBS buffer (pH 7.4) for 1 h at room temperature in pH 7.4 PBS buffer, followed by three rinse steps to remove the non-reacted antibody.

4.5. Release of cell-backpacks conjugates directly from the glass slide

Cell incubation protocol example can be found in work published by our group [16,52]. Briefly, the slide is cut and placed in the bottom of a well in a 6-well plate or a small Petri dish. 2 mL of cells suspended in appropriate media (~106 cells/mL) are pipetted onto the surface. The entire plate is agitated for 15 min at 37 °C, followed by 37 °C incubation for 15 min, and this cycle is repeated identically once more. The glass slide, now containing cells attached to surface-bound patches, is removed and gently shaken for ~15 s upside down in 37 °C PBS to remove all cells not attached to a patch.

In this case, to release the cell-backpacks, 1 mL of 100 mM of melibiose in PBS was added to the top of the glass slide and incubated for 1 h at 37 °C. These solutions were then pipetted up and down to release the cell-backpacks from the glass slide. Additionally a cell scraper is used to help remove the cell-backpack conjugates from the glass slide.

4.6. Backpacks thickness

Backpacks thicknesses were measured using a profilometer (Tecan).

4.7. Backpacks and PAH/CAT films activity

Catalase activity inside backpacks and PAH/CAT films was assayed by incubating the samples with hydrogen peroxide solution. A piece of ~1 cm^2 of a glass slide containing the backpacks or the PAH/CAT films was placed inside a 20 mL glass vial containing a 3 mL of a 15 mmol solution of H_2O_2 diluted in PBS. Samples were agitated (150 rpm) for 2 min and then most of the solution of H_2O_2 was transferred to a quartz cuvette (optical path length of 1 cm) and the absorbance read at 240 nm. The solution was then placed back inside the original vial and re-analyzed every 2 min until 4 or 5 time points were collected. The slope of the consumption of H_2O_2 was then used to calculate the activity of the enzyme (U/area), by using the following equation [53]. The test was run in triplicate. The areas of glass slide pieces were measured for normalization.

$$\text{Activity} = dA/dt * V/(A * b * \varepsilon) \quad (1)$$

where dA/dt is the change in the absorbance with respect to time, V is the total volume of hydrogen peroxide and PBS used, A is the area of the glass slide piece, b is the optical path length of the cuvette and ε is the extinction coefficient for the hydrogen peroxide. The extinction coefficient is calculated from the slope of a H_2O_2 calibration curve, in this case ε was equal to 43.6 $M^{-1}cm^{-1}$. The areas of each slide were normalized to plot the average activity of the slides over time, and the percent of the activity remaining relative to the controls.

4.8. Protease challenge test

Samples were cut from the slide into approximately 1 cm [2] pieces and placed in 20 mL glass vials. The areas were measured for normalization. Two of the pieces of backpacks samples were incubated in 3 mL of protease solution (3.3 mg/mL in PBS), and one sample was used as a control (incubated in 3 mL of PBS). Samples were incubated in protease solution (37 °C) for 30 min, 1 h, 1 h30 min, and 2 h. Once the desired incubation time was completed, samples were rinsed thoroughly in PBS solution to remove excess of protease, and then placed in vials containing 5mL of hydrogen peroxide solution (15 mM in PBS). For time point zero (no protease incubation, control) samples were immediately tested after adding hydrogen peroxide solution. Once in a hydrogen peroxide solution, absorbance decay of hydrogen peroxide was measured overtime at 240 nm, by measuring the absorbance of each sample about every 2 min for about 10 min, recording the time, sample, and absorbance. To measure the absorbance, solution from the glass vial was carefully poured into a quartz cuvette, and then poured back into the vial after each reading. Samples were agitated at 150 rpm between readings. Absorbance values were plotted versus time to find the slope. This procedure allowed calculating the activity of the pieces of slide using Equation (1).

4.9. Catalase release from backpacks

CAT backpacks were incubated in PBS solution, at 37 °C and samples of the supernatant were collected over time (up to 72 h). Micro BCA analyses were performed in order to look for catalase in solution.

4.10. Cell culture

A human colon epithelium cell line, Caco-2, (ATCC CCL-17), mouse transformed endothelium cell line, b.End 3 (ATCC® CRL-2299)), and mouse macrophage cell line RAW 264.7 (ATCC TIB-71) were cultured in Dulbecco's Modified Eagle's Media (DMEM, Invitrogen, Carlsbad, CA, USA) supplemented with 10% FBS, 10 mM HEPES and penicillin/streptomycin.

To obtain bone marrow-derived macrophages (BMM), cells were extracted from femurs of C57/BL male mice [54] and cultured for 12–14 days in DMEM medium (Invitrogen, Carlsbad, CA) supplemented with 1000 U/mL macrophage colony-stimulating factor (MCSF).

4.11. Loading macrophages with cell backpacks

A half of glass slide with cell backpacks attached was placed into 6-well plate, and supplemented with 500 μl NeutrAvidin Dylight 550 (50 μg/mL final concentration) in pH 7.4 PBS buffer for 1 h at 4 °C. Then, the glass slide was rinsed 3× in PBS, and backpacks were incubated with biotinylated CD11b antibody (50 μg/mL) diluted with PBS buffer (pH 7.4) for 1 h at room temperature in pH 7.4 PBS buffer. Following incubation, the glass slide was rinsed 3× with PBS to remove the non-reacted antibody, and DIO-labeled Raw 264.7 macrophages (green) suspended in 2 mL media (~2×10^6 cells/mL) were pipetted onto the surface of the glass slide with backpacks and covered with foil. The entire plate was agitated for 15 min at 37 °C, followed by 37 °C incubation for 15 min, and this cycle was repeated

identically once more. Then, the glass slide, containing cells attached to surface-bound patches was washed 3× with media to remove all cells not attached to a patch, and red backpacks on the slide with green cells attached were examined with fluorescent microscope (Supplemental Fig. 4). 1 mL of 100 mM of melibiose in PBS was added to the plate on top of the glass slide and incubated for 1 h at 37 °C in the incubator to detach cell-carriers with backpacks from the glass slide. Then, the cells were detached by pipetting them up and down and utilized in subsequent studies.

4.12. Antioxidant activity measurements

Catalytic activity of catalase alone or incorporated into call patches was measured by two methods: spectrophotometry and Amplex Red assay. In cell-free system, catalase activity was measured by hydrogen peroxide decomposition method as described earlier [36]. The initial activity was 38,000 U/mg protein for catalase. The concentration dependence of enzymatic activity as well as catalase stability was studied in a range of 1.7–35.2 mM hydrogen peroxide, and expressed in residual activity *vs.* Initial activity of catalase in the backpacks.

The decomposition of ROS by catalase released from backpacks in pre-activated macrophages was evaluated by CellROX Green Reagent fluorescence assay (Molecular probes) as described earlier [55]. Briefly, various doses of catalase-loaded cell backpacks (1.3×10^6 backpacks/ml; 1.3×10^5 backpacks/ml; 1.3×10^4 backpacks/ml; or 1.3×10^3 backpacks/ml) were added to activated macrophages for 18 h. Following incubation, the supernatants were supplemented with CellROX Green Reagent (stock solution was diluted in assay buffer 25 times, and 50 μl of working solution was added to the fresh plate with 50 μl media from the cells for 1 h). The decomposition of free radicals by catalase released from backpacks was measured by fluorescence at $\lambda_{ex}/\lambda_{em}$ = 490 nm/520 nm.

4.13. Macrophage adherence and migratory activities

It is known that immune cells utilize various integrins, in particular α-4 integrin to passage into the central nervous system (CNS) [56]. Therefore, we investigated whether attachment of catalase-loaded patches affect macrophage ability to adhere and migrate *in vitro* model of BBB as described earlier [57]. Macrophages were incubated with backpacks loaded with catalase. After the incubation macrophages were stained with phycoerythrin (PE)-conjugated anti-CD49d antibodies; and PE-Cy5-conjugated nonspecific antibodies as isotype control. Migratory activities were investigated in two *in vitro* models of BBB: confluent monolayers of bEnd 3 and Caco-2 cells that were grown on polycarbonate inserts [57]. The procedure was described in[19]. FITC-labeled Raw 264.7 macrophages (green) were loaded with fluorescently-labeled backpacks (red) backpacks as described above. Cell-free backpacks were used as a control. We utilized macrophage chemotactic factor-1 (MCP-1) as a chemoattractant [19]. Following the incubation at several times (1 h, 4 h, and 14 h) at 37 °C in a shaker, the cell inserts were removed, and centrifuged for 10 min at 400*g* to pellet the migrating cells with cell backpacks or backpacks alone to the plate's bottom chamber. For adherence studies, BBB monolayers were grown on 24-well plates as described [57]. Macrophages labeled with Alexa Fluor 680, were loaded with backpacks, and added to BBB

cell monolayers. Non-loaded BMM were used as a control. The amount of Alexa Fluor-labeled macrophages was measured determined as described in Ref. [58].

4.14. Animals

Male C57/BL mice (Charles River Laboratories, USA) 8 weeks of age were used in experiments demonstrating brain targeting by macrophages with cell backpacks. The animals were kept five per cage with an air filter cover under light- (12-h light/dark cycle) and temperature-controlled (22 ± 1 °C) environment. All manipulations with the animals were performed under a sterilized laminar hood. Food and water were given *ad libitum*. The animals were treated in accordance to the *Principles of Animal Care* outlined by National Institutes of Health and approved by the Institutional Animal Care and Use Committee of the University of North Carolina at Chapel Hill.

4.15. Confocal microscopy

To utilize confocal imaging, macrophages were labeled with a fluorescent dye DiO [27]. For *in vitro* investigations, DiO-labeled Raw 264.7 macrophages with fluorescently-labeled back packs attached were seeded to the chamber slides and examined by confocal microscope. For *in vivo* investigations, C57/BL mice with brain inflammation caused by LPS intracranial injections (10 μg LPS in 0.9% NaCl with 0.02% ascorbic acid, flow rate of 0.1 μL/min into the striatum (AP: +0.5; L: −2.0 and DV: −3.0 mm)) were used. Twenty four hours later, macrophages (green) with backpacks (red) attached were systemically injected into LPS-intoxicated mice (5 mice/group, three independent experiments). Fourteen hours later, mice were sacrificed, perfused according to standard protocol; brain slides were sectioned, and examined by confocal fluorescence microscopy. Mice injected with cell-free backpacks were used as a control group (5 mice/group). To examine effect of cell patches attachment to macrophages, another control group of mice was injected with non-loaded macrophages.

4.16. Statistical analysis

To investigate for statistical significance of the obtained results, a one-way ANOVA with multiple comparisons using GraphPad Prism 6.0 was used. A significance level was chosen at a minimum p value of 0.05.

Supplementary Material

Refer to Web version on PubMed Central for supplementary material.

Acknowledgments

This work was supported in part by the MRSEC Program of the National Science Foundation under award number DMR-0819762. Grant No. R01 NS057748 awarded by the National Institutes of Health. R.J.G.N. was funded by Brazilian Federal Agency for Support and Evaluation of Graduate Education (CAPES) under award number 88888.996640/2014-00.

References

1. Mason C, Brindley DA, Culme-Seymour EJ, Davie NL. Cell therapy industry: billion dollar global business with unlimited potential. Regen. Med. 2011; 6:265–272. http://dx.doi.org/10.2217/rme.11.28. [PubMed: 21548728]

2. Daneman R. The blood-brain barrier in health and disease. Ann. Neurol. 2012; 72:648–672. http://dx.doi.org/10.1002/ana.23648. [PubMed: 23280789]
3. Anthony DC, Bolton SJ, Fearn S, Perry VH. Age-related effects of interleukin-1 beta on polymorphonuclear neutrophil-dependent increases in blood-brain barrier permeability in rats. Brain. 1997; 120(Pt 3):435–444. [PubMed: 9126055]
4. Anthony DC, Blond D, Dempster R, Perry VH. Chemokine targets in acute brain injury and disease. Prog. Brain Res. 2001; 132:507–524. [PubMed: 11545015]
5. Blamire AM, et al. Interleukin-1beta -induced changes in blood-brain barrier permeability, apparent diffusion coefficient, and cerebral blood volume in the rat brain: a magnetic resonance study. J. Neurosci. 2000; 20:8153–8159. [PubMed: 11050138]
6. Persidsky Y, et al. Microglial and astrocyte chemokines regulate monocyte migration through the blood-brain barrier in human immunodeficiency virus-1 encephalitis. Am. J. Pathol. 1999; 155:1599–1611. [PubMed: 10550317]
7. Pawlowski NA, Kaplan G, Abraham E, Cohn ZA. The selective binding and transmigration of monocytes through the junctional complexes of human endothelium. J. Exp. Med. 1988; 168:1865–1882. [PubMed: 3183575]
8. Lossinsky AS, Shivers RR. Structural pathways for macromolecular and cellular transport across the blood-brain barrier during inflammatory conditions. Rev. Histol. Histopathol. 2004; 19:535–564.
9. Kuby, J. Immunology. Freeman, WH. Co.; 1994.
10. Batrakova EV, Gendelman HE, Kabanov AV. Cell-mediated drug delivery. Expert Opin. Drug Deliv. 2011; 8:415–433. http://dx.doi.org/10.1517/17425247.2011.559457. [PubMed: 21348773]
11. Saraiva C, et al. Nanoparticle-mediated brain drug delivery: overcoming blood–brain barrier to treat neurodegenerative diseases. J. Contr. Release. 2016; 235:34–47. http://dx.doi.org/10.1016/j.jconrel.2016.05.044.
12. Doshi N, et al. Cell-based drug delivery devices using phagocytosis-resistant backpacks. Adv. Mater. 2011; 23:H105–H109. http://dx.doi.org/10.1002/adma.201004074. [PubMed: 21365691]
13. Swiston AJ, Gilbert JB, Irvine DJ, Cohen RE, Rubner MF. Freely suspended cellular “backpacks” lead to cell aggregate self-assembly. Biomacromolecules. 2010; 11:1826–1832. http://dx.doi.org/10.1021/bm100305h. [PubMed: 20527876]
14. Swiston AJ, et al. Surface functionalization of living cells with multilayer patches. Nano Lett. 2008; 8:4446–4453. http://dx.doi.org/10.1021/nl802404h. [PubMed: 19367972]
15. Anselmo, AC., et al. Monocyte-mediated delivery of polymeric backpacks to inflamed tissues: a generalized strategy to deliver drugs to treat inflammation. J. Contr. Release. doi:http://dx.doi.org/10.1016/j.jconrel.2014.11.027
16. Polak R, et al. Liposome-loaded cell backpacks. Adv. Healthc. Mater. 2015; 4:2832–2841. http://dx.doi.org/10.1002/adhm.201500604. [PubMed: 26616471]
17. Xia J, et al. Catalase-laden microdevices for cell-mediated enzyme delivery. Langmuir. 2016; 32:13386–13393. http://dx.doi.org/10.1021/acs.langmuir.6b03160. [PubMed: 27793069]
18. Polak R, et al. Sugar-mediated disassembly of mucin/lectin multilayers and their use as pH-tolerant, on-demand sacrificial layers. Biomacromolecules. 2014; 15:3093–3098. http://dx.doi.org/10.1021/bm5006905. [PubMed: 24964165]
19. Zelivyanskaya ML, et al. Tracking superparamagnetic iron oxide labeled monocytes in brain by high-field magnetic resonance imaging. J. Neurosci. Res. 2003; 73:284–295. [PubMed: 12868062]
20. Lise-Marie L, Don H, Shouheng S. Magnetic nanoparticles as both imaging probes and therapeutic agents. Curr. Top. Med. Chem. 2010; 10:1184–1197. http://dx.doi.org/10.2174/156802610791384207. [PubMed: 20388109]
21. Jianxin W, et al. Magnetic nanoparticles for MRI of brain tumors. Curr. Pharm. Biotechnol. 2012; 13:2403–2416. http://dx.doi.org/10.2174/138920112803341824. [PubMed: 23016645]
22. Mahmoudi K, Hadjipanayis CG. The application of magnetic nanoparticles for the treatment of brain tumors. Front. Chem. 2014; 2 http://dx.doi.org/10.3389/fchem.2014.00109.
23. Klyachko NL, et al. Macrophages offer a paradigm switch for CNS delivery of therapeutic proteins. Nanomedicine. 2014; 9:1403–1422. http://dx.doi.org/10.2217/nnm.13.115. [PubMed: 24237263]

24. Batrakova EV, et al. A macrophage-nanozyme delivery system for Parkinson's disease. Bioconjugate Chem. 2007; 18:1498–1506. http://dx.doi.org/10.1021/bc700184b.
25. Brynskikh AM, et al. Macrophage delivery of therapeutic nanozymes in a murine model of Parkinson's disease. Nanomedicine. 2010; 5:379–396. http://dx.doi.org/10.2217/nnm.10.7. [PubMed: 20394532]
26. Zhao Y, et al. Active targeted macrophage-mediated delivery of catalase to affected brain regions in models of Parkinson's disease. J. Nanomed. Nanotechnol. 2011; S4 http://dx.doi.org/10.4172/2157-7439.S4-003.
27. Haney MJ, et al. Specific transfection of inflamed brain by macrophages: a new therapeutic strategy for neurodegenerative diseases. PLoS one. 2013; 8:e61852. [PubMed: 23620794]
28. Hsu BB, Park M-H, Hagerman SR, Hammond PT. Multimonth controlled small molecule release from biodegradable thin films. Proc. Natl. Acad. Sci. 2014; 111:12175–12180. http://dx.doi.org/10.1073/pnas.1323829111. [PubMed: 25092310]
29. Hsu BB, et al. Multifunctional self-assembled films for rapid hemostat and sustained anti-infective delivery. ACS Biomater. Sci. Eng. 2015; 1:148–156. http://dx.doi.org/10.1021/ab500050m.
30. Hsu BB, et al. Clotting mimicry from robust hemostatic bandages based on self-assembling peptides. ACS Nano. 2015; 9:9394–9406. http://dx.doi.org/10.1021/acsnano.5b02374. [PubMed: 26284753]
31. Mandapalli, PK., et al. Layer-by-layer thin films for co-delivery of TGF-β siRNA and epidermal growth factor to improve excisional wound healing; AAPS Pharm Sci Tech. 2016. p. 1-12.http://dx.doi.org/10.1208/s12249-016-0571-6
32. Saurer EM, Flessner RM, Sullivan SP, Prausnitz MR, Lynn DM. Layer-by-layer assembly of DNA- and protein-containing films on microneedles for drug delivery to the skin. Biomacromolecules. 2010; 11:3136–3143. http://dx.doi.org/10.1021/bm1009443. [PubMed: 20942396]
33. Cho Y, Lee JB, Hong J. Controlled release of an anti-cancer drug from DNA structured nano-films. Sci. Rep. 2014; 4:4078. http://dx.doi.org/10.1038/srep04078. http://www.nature.com/articles/srep04078#supplementaryinformation. [PubMed: 24518218]
34. Caruso F, Trau D, Möhwald H, Renneberg R. Enzyme encapsulation in layer-by-layer engineered polymer multilayer capsules. Langmuir. 2000; 16:1485–1488. http://dx.doi.org/10.1021/la991161n.
35. Such GK, Johnston APR, Caruso F. Engineered hydrogen-bonded polymer multilayers: from assembly to biomedical applications. Chem. Soc. Rev. 2011; 40:19–29. http://dx.doi.org/10.1039/c0cs00001a. [PubMed: 20882254]
36. Zhao Y, et al. Polyelectrolyte complex optimization for macrophage delivery of redox enzyme nanoparticles. Nanomedicine Lond. 2011; 6:25–42. http://dx.doi.org/10.2217/nnm.10.129. [PubMed: 21182416]
37. Bachis A, Mocchetti I. Brain-derived neurotrophic factor is neuroprotective against human immunodeficiency virus-1 envelope proteins. Ann. N. Y. Acad. Sci. 2005; 1053:247–257. [PubMed: 16179530]
38. Ying Wang J, et al. Neuroprotective effects of IGF-I against TNFalpha-induced neuronal damage in HIV-associated dementia. Virology. 2003; 305:66–76. [PubMed: 12504542]
39. Koliatsos VE, et al. Human nerve growth factor prevents degeneration of basal forebrain cholinergic neurons in primates. Ann. Neurol. 1991; 30:831–840. [PubMed: 1789695]
40. Dogrukol-Ak D, Banks WA, Tuncel N, Tuncel M. Passage of vasoactive intestinal peptide across the blood-brain barrier. Peptides. 2003; 24:437–444. [PubMed: 12732342]
41. Perry VH, Bell MD, Brown HC, Matyszak MK. Inflammation in the nervous system. Curr. Opin. Neurobiol. 1995; 5:636–641. [PubMed: 8580715]
42. McGeer PL, Itagaki S, Boyes BE, McGeer EG. Reactive microglia are positive for HLA-DR in the substantia nigra of Parkinson's and Alzheimer's disease brains. Neurology. 1988; 38:1285–1291. [PubMed: 3399080]
43. Busciglio J, Yankner BA. Apoptosis and increased generation of reactive oxygen species in Down's syndrome neurons in vitro. Nature. 1995; 378:776–779. [PubMed: 8524410]
44. Ebadi M, Srinivasan SK, Baxi MD. Oxidative stress and antioxidant therapy in Parkinson's disease. Prog. Neurobiol. 1996; 48:1–19. [PubMed: 8830346]

45. Wu DC, et al. NADPH oxidase mediates oxidative stress in the 1-methyl-4-phenyl-1,2,3,6-tetrahydropyridine model of Parkinson's disease. Proc. Natl. Acad. Sci. U. S. A. 2003; 100:6145–6150. [PubMed: 12721370]
46. Haney MJ, et al. Cell-mediated transfer of catalase nanoparticles from macrophages to brain endothelial, glial and neuronal cells. Nanomedicine (Lond). 2011; 6:1215–1230. http://dx.doi.org/10.2217/nnm.11.32. [PubMed: 21449849]
47. Klyachko NL, et al. Cross-linked antioxidant nanozymes for improved delivery to CNS. Nanomedicine Nanotechnol. Biol. Med. 2012; 8:119–129. http://dx.doi.org/10.1016/j.nano.2011.05.010 doi:S1549-9634(11)00182-1 [pii].
48. Haney MJ, et al. Blood-borne macrophage-neural cell interactions hitchhike endosome networks for cell-based nanozyme brain delivery. Nanomedicine (Lond). 2012; 7:815–833. http://dx.doi.org/10.2217/nnm.11.156. [PubMed: 22236307]
49. Zhao Y, et al. GDNF-transfected macrophages produce potent neuroprotective effects in Parkinson's disease mouse model. PLoS One. 2014; 9:e106867. http://dx.doi.org/10.1371/journal.pone.0106867. [PubMed: 25229627]
50. Maruyama W, et al. Neuroprotection by propargylamines in Parkinson's disease: suppression of apoptosis and induction of prosurvival genes. Neurotoxicol Teratol. 2002; 24:675–682. [PubMed: 12200198]
51. Swiston A, Gilbert J, Irvine D, Cohen R, Rubner M. Injectable cellular “Backpacks” lead to cell aggregate self-assembly. Abstr. Pap. Am. Chem. Soc. 2010; 240
52. Anselmo AC, et al. Monocyte-mediated delivery of polymeric backpacks to inflamed tissues: a generalized strategy to deliver drugs to treat inflammation. J. Control Release. 2015; 199:29–36. http://dx.doi.org/10.1016/j.jconrel.2014.11.027. [PubMed: 25481443]
53. Aebi H. Catalase in vitro. Methods Enzymol. 1984; 105:121–126. [PubMed: 6727660]
54. Dou H, et al. Development of a macrophage-based nanoparticle platform for antiretroviral drug delivery. Blood. 2006; 108:2827–2835. [PubMed: 16809617]
55. Batrakova EV, et al. A macrophage-nanozyme delivery system for Parkinson's disease. Bioconjug Chem. 2007; 18:1498–1506. http://dx.doi.org/10.1021/bc700184b. [PubMed: 17760417]
56. Seguin R, Biernacki K, Rotondo RL, Prat A, Antel JP. Regulation and functional effects of monocyte migration across human brain-derived endothelial cells. J. Neuropathol. Exp. Neurol. 2003; 62:412–419. [PubMed: 12722833]
57. Batrakova E, Han H, Miller D, Kabanov A. Effects of pluronic P85 unimers and micelles on drug permeability in polarized BBMEC and Caco-2 cells. Pharm. Res. 1998; 15:1525–1532. [PubMed: 9794493]
58. Batrakova E, Li S, Miller D, Kabanov A. Pluronic P85 increases permeability of a broad spectrum of drugs in polarized BBMEC and Caco-2 cell monolayers. Pharm. Res. 1999; 16:1366–1372. [PubMed: 10496651]

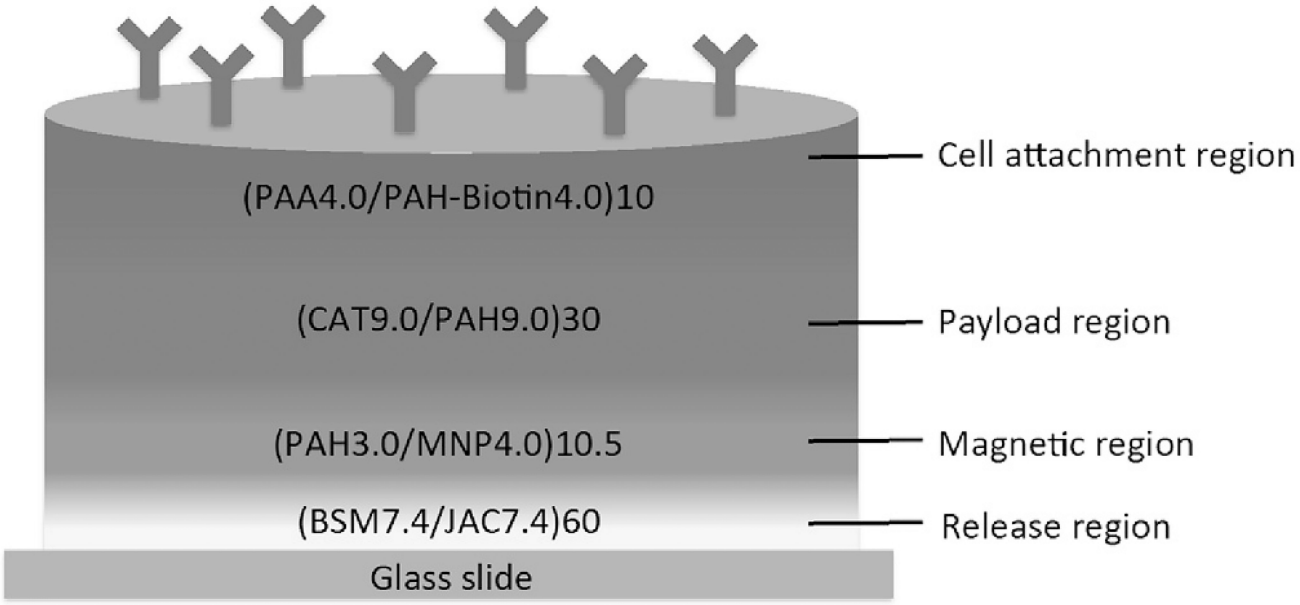

Fig. 1.

Scheme showing the catalase containing backpack structure. From bottom to top: Release region is composed of 60 bilayers of bovine submaxillary mucin (BSM) and lectin jacalin (JAC); Magnetic region made of 10.5 bilayers of poly(allylamine hydrochloride) (PAH) and magnetic nanoparticles (MNP); Payload region containing 30 bilayers of PAH and catalase from bovine liver (CAT); Cell attachment region comprised of 10 bilayers of poly(acrylic aid) (PAA) and biotinylated PAH (PAH-biotin). Backpacks are topped with CD11b antibodies for macrophage conjugation.

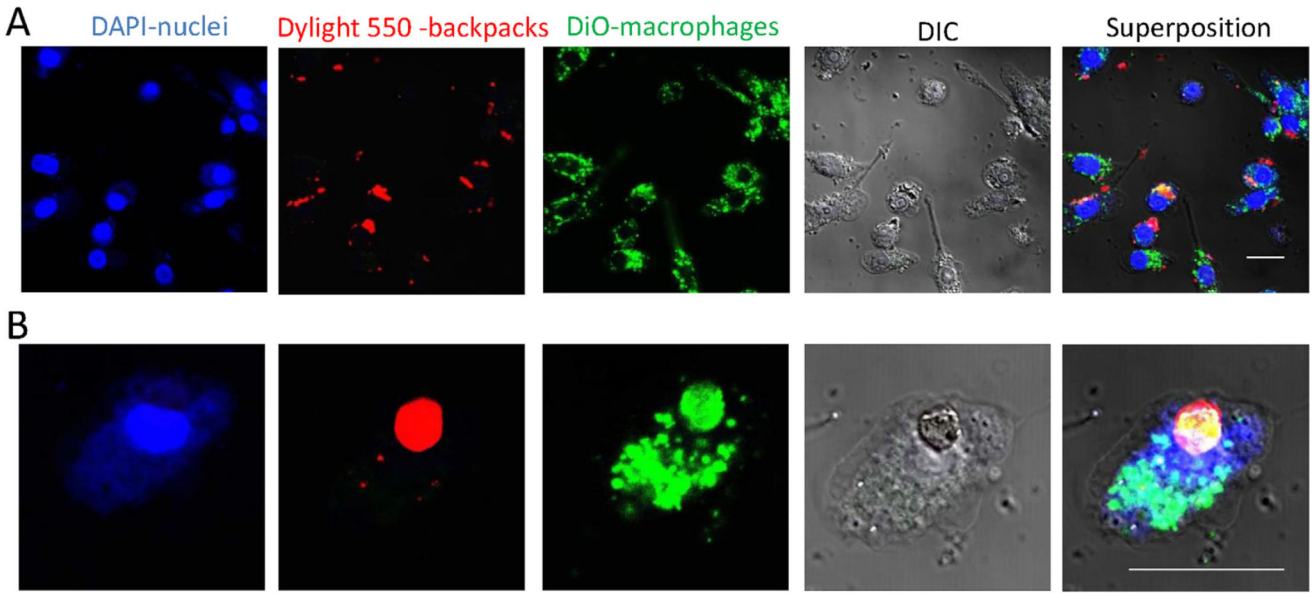

Fig. 2.

Macrophages with attached backpacks *in vitro*. **A**: 40× magnification; **B**: 2× zoom 63× magnification. The bar: 20 μM. Macrophage nuclei are stained in blue (DAPI); backpacks are stained in red (Neutravidin Dylight 550); macrophages are stained with DiO (green). (For interpretation of the references to colour in this figure legend, the reader is referred to the web version of this article.)

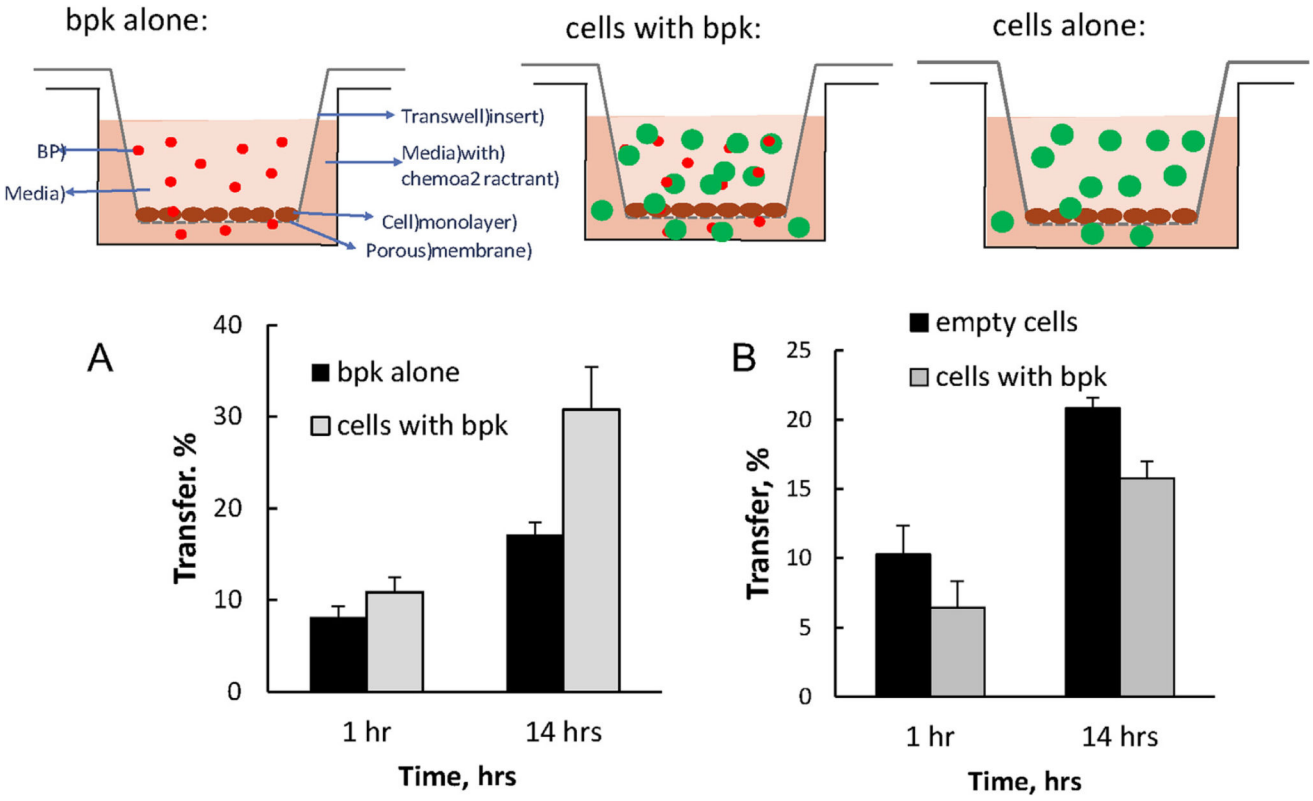

Fig. 3.

In vitro assay of the translocation of macrophages, cell-backpacks, and macrophage-backpack conjugates across cell monolayers. The cartoon illustrates the ability for backpacks alone (upper left scheme), macrophage-backpack conjugates (center scheme) or macrophages alone (upper right scheme) to cross a cell monolayer *in vitro*. **A**) Macrophage-mediated transport of backpacks across the BBB *in vitro*; **B**) Macrophage transfer across the BBB *in vitro*. **A**: Fluorescently-labeled backpacks loaded onto non-labeled macrophages (red bars) or cell-free backpacks (black bars) were added to a donor chamber of bEnd.3 cell monolayers seeded onto inserts. **B**: Fluorescently- labeled macrophages with attached backpacks (green bars) or non-loaded “free” cells (black bars) were added to a donor chamber of bEnd.3 cell monolayers seeded onto inserts. Following different time points, the media from the receiver chamber was collected and examined for the amount of backpacks (**A**) or macrophages (**B**) transferred across the cell monolayers. (For interpretation of the references to colour in this figure legend, the reader is referred to the web version of this article.)

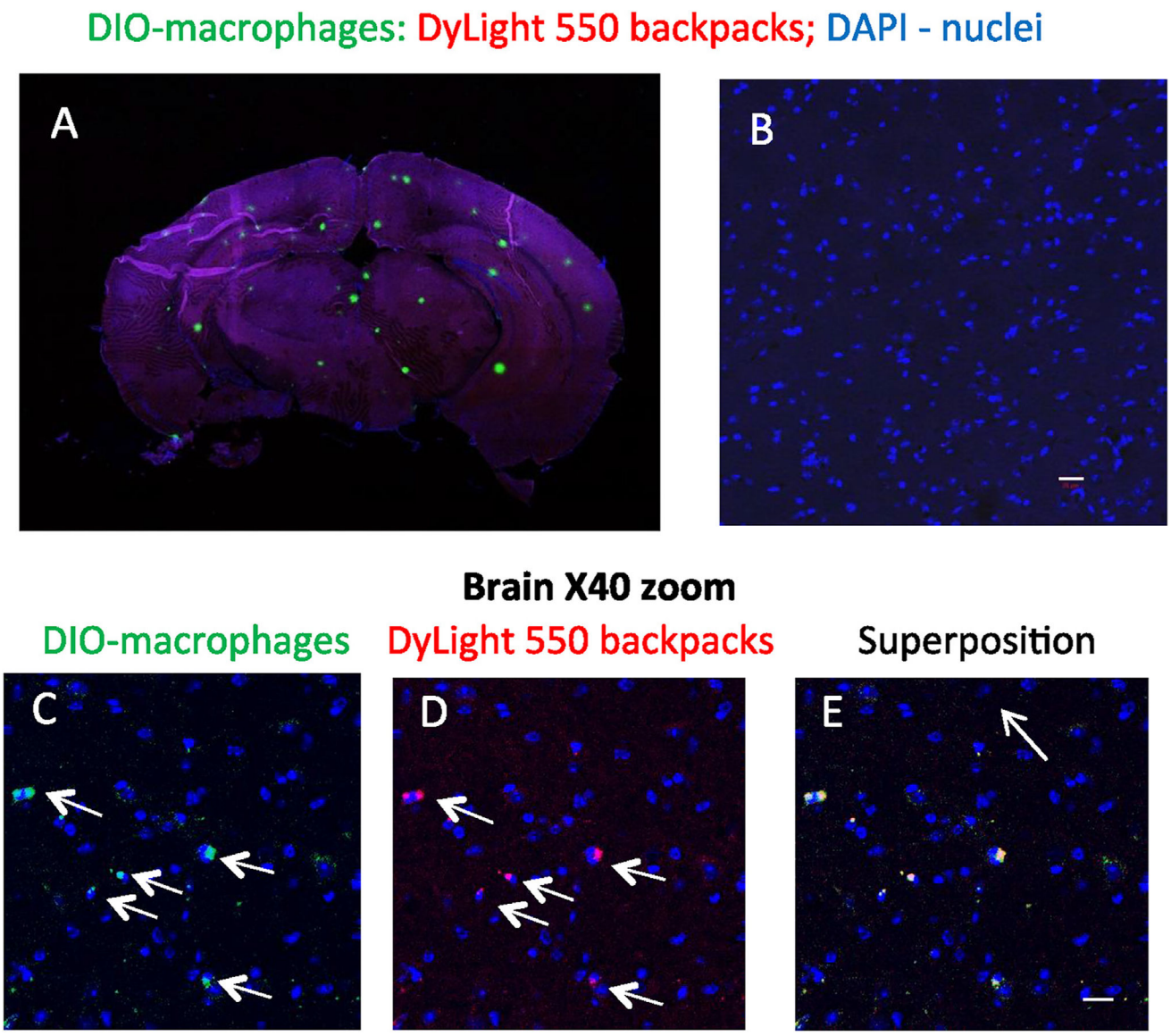

Fig. 4. Recruitment of macrophages with the attached backpacks to the brain in LPS-intoxicated mice

Fluorescently-labeled DiO-macrophages (green, 2×10^6 cells/ml) loaded with fluorescently-labeled backpacks (red, NeutrAvidin 550) attached. Cell-backpacks (5×10^6 cells/mouse in 100 μl) were injected into C57/BL mice (5 mice/group) with brain inflammation (**A, C–E**). Fourteen hours later, mice were sacrificed, and brain slides were examined by confocal microscopy (**A**: whole brain, **B–E**: 40× magnification). LPS-intoxicated mice injected with backpacks alone (no cell-carriers, 5 mice/group) were used as a control group (**B**). Co-localization of fluorescently-labeled macrophages (green, **C**) and backpacks (red, **D**) manifested in yellow staining (**E**) confirmed that macrophages delivered considerable amount of backpacks to the inflamed brain (shown by arrows). No fluorescence was found in the inflamed brain when backpacks were injected alone (without cell-carriers, **B**) indicating that systemically administered macrophages facilitated transport of backpacks across the BBB in the presence of brain inflammation. The representative images from three

independent experiments. The bar: 20 μm. (For interpretation of the references to colour in this figure legend, the reader is referred to the web version of this article.)

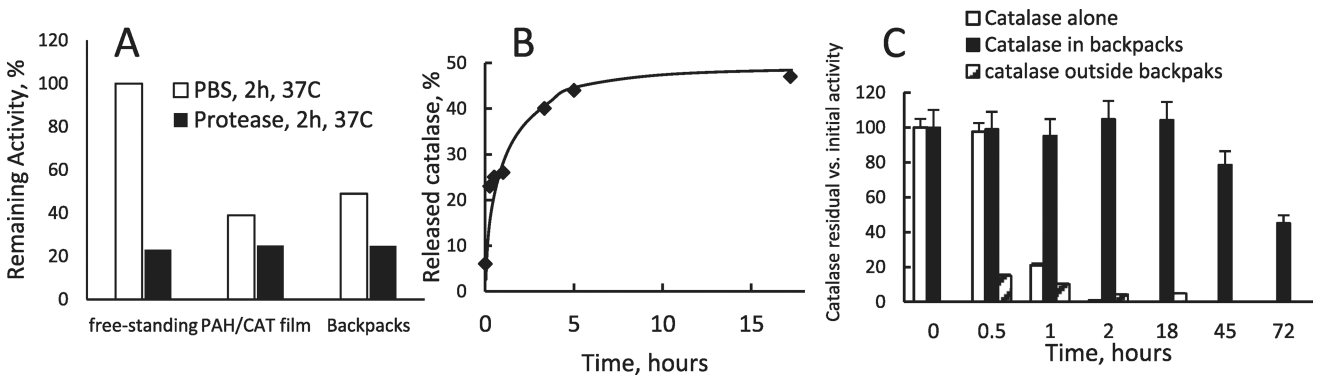

Fig. 5.

Characterization of catalase incorporated into cell backpacks. **A)** Protease challenge test: free-standing catalase in solution, payload region films (PAH9.0/CAT9.0)30.5, and catalase containing backpacks had their activity measured before and after incubated in PBS (control) or in protease solution for 2 h, 37 °C. Remaining of activity (%) was calculated relative to time zero incubation time (initial activity). **B)** Activity of catalase released from backpacks was measured using hydrogen peroxide decomposition by monitoring the change in absorbance at 240 nm (the extinction coefficient of H_2O_2 is 44 $M^{-1}cm^{-1}$) [36]. **C**) Loading of catalase into backpacks increased stability of the enzyme against a mixture of proteinases (trypsin and pronase). Contrary to the free catalase (white bars) that was completely inactivated by proteinases after 2 h, backpack-incorporated catalase remained active for more than 72 h.

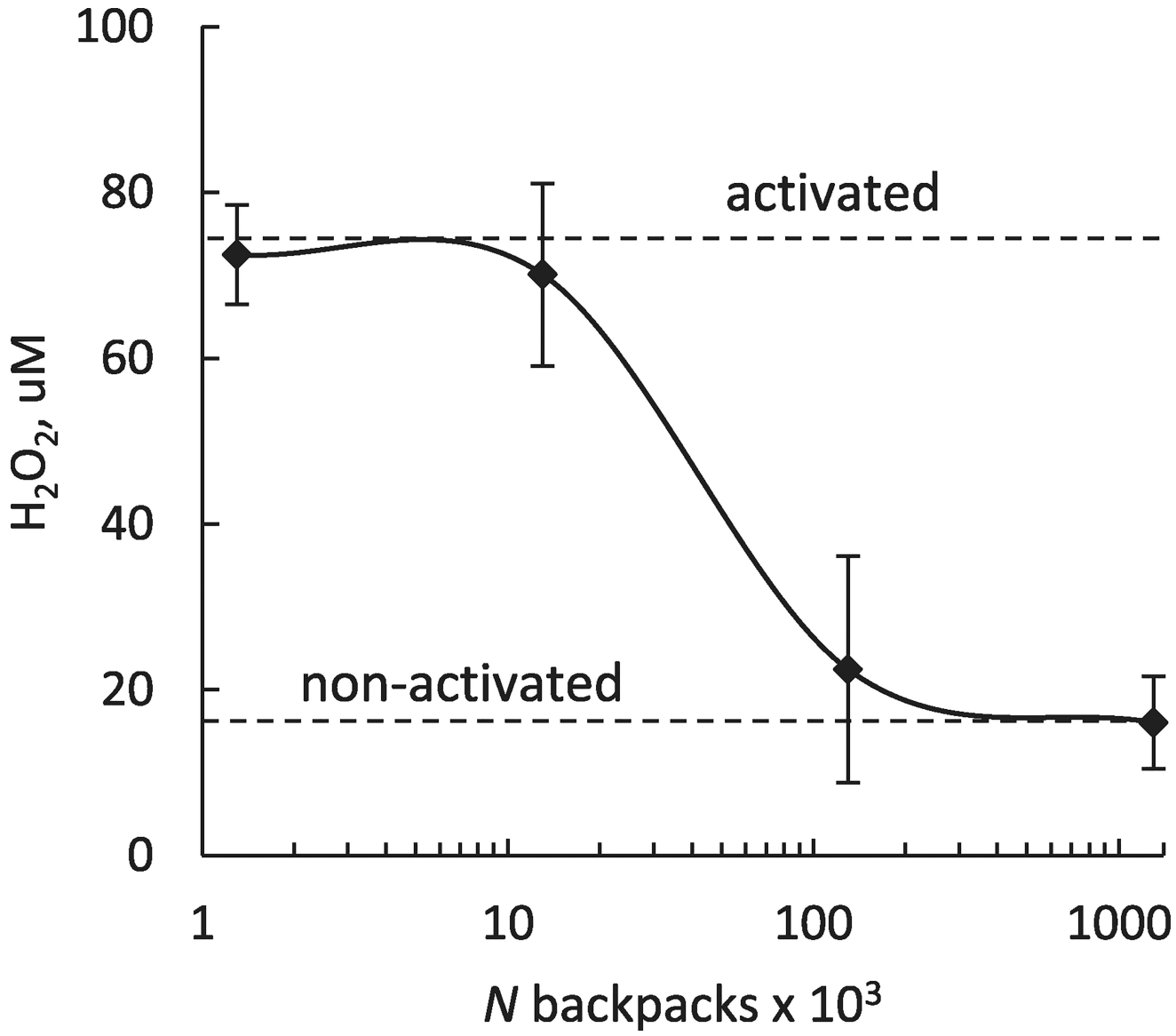

Fig. 6. Antioxidant activity of catalase-loaded backpacks in activated macrophages

RAW 264.7 macrophages were activated with 100 μg/ml LPS overnight. 24 h later, various amount of catalase-loaded backpacks were added to the cells and the levels of ROS in call were measured. Catalase in higher doses of backpacks efficiently decreased ROS produced by activated macrophages to the levels in non-activated cells.